Antiproton, proton and electron impact multiple ionization of rare gases

2012 J. Phys. B: At. Mol. Opt. Phys. 45 105201

(http://iopscience.iop.org/0953-4075/45/10/105201)

J. Phys. B: At. Mol. Opt. Phys. **45** (2012) 105201 (15pp) doi:10.1088/0953-4075/45/10/105201

Antiproton, proton and electron impact multiple ionization of rare gases

C C Montanari and J E Miraglia

Instituto de Astronomía y Física del Espacio, CONICET and Univesridad de Buenos Aires, Casilla de Correo 67, Sucursal 28, C1428EGA, Buenos Aires, Argentina

E-mail: mclaudia@iafe.uba.ar

Received 13 January 2012, in final form 9 April 2012
Published 3 May 2012
Online at stacks.iop.org/JPhysB/45/105201

Abstract

We present a study on multiple ionization of Ne, Ar, Kr and Xe by antiproton, proton and electron impact. Four different aspects are involved in this work. First, the theoretical calculations of ionization probabilities by impact of antiprotons and protons, in an extended energy region (25 keV to 10 MeV), using the continuum distorted-wave eikonal initial state approximation and the first Born approximation. Second, the inclusion of Auger-type post-collisional contributions through experimental photoionization branching ratios. These contributions to multiple ionization are very important in the high-energy region. Third, the comparison with the available experimental data on multiple ionization by protons and antiprotons in the extended energy range, and by electrons for high-impact velocities, where proton, antiproton and electron impact results are expected to converge. It is also the energy region where direct ionization does not explain the experimental results, and the post-collisional ionization is the main contribution to multiple ionization. And fourth, total ionization cross sections are calculated and compared with the antiproton, proton and electron experimental data, showing the importance of Auger-type multiple ionization for heavy targets even at the level of total cross sections. Gross and count cross sections are scrutinized.

(Some figures may appear in colour only in the online journal)

1. Introduction

Multiple ionization is one of the most challenging subjects within the field of atomic collisions, being a sensitive test for both, theoretical and experimental research.

Experimental measurements on multiple ionization require highly advanced techniques to get absolute measurements of all possible channels and final states. For positive ions they must separate pure ionization from capture channels, which enhance the data in the intermediate energy region [1]. Pioneering on the research on multiple ionization of rare gases by positive ions are the works by DuBois, Manson and co-workers in the 1980s [2–6]. There are some reviews that compile the experimental and theoretical knowledge on this subject [7–9].

The case of antiproton impact is quite different. Despite the experimental difficulty to achieve a low-energy antiproton beam, they are the cleanest and possibly the simplest ionization dynamics to describe [10], as there are no possible capture channels or electron exchanges to consider; ionization is then just pure ionization. On the other hand, the study of antiproton impact ionization is very interesting in itself, considering that they are projectiles produced in high-energy physics sources.

Antiproton facilities for atomic physics have been available only in the last 25 years [11]. Experimental research on antiproton impact ionization has been developed by Knudsen and co-workers, at the University of Aarhus, together with the collaborators working at CERN, first in the Low Energy Antiproton Ring (LEAR) and nowadays at the Antiproton Decelerator (AD). For multiple ionization, see for example [11–16]. Classical reviews on particle and antiparticle collisions can be found in [17, 18]. A very recent *state of the art* of antiproton impact ionization has been published by Kirchner and Knudsen [10].

Multiple ionization is also a subject of interest in electron impact ionization [19, 20]. In fact, the amount of experimental measurements on multiple ionization by electron impact is much greater than that of the different positive ions or antiprotons. Pioneering in this area are the works by Schram and co-workers in the 1960s [21–23], Krishnakumar and

Srivastava [24], Nagy *et al* [25], covering an extended energy region from tens of eV to tens of keV.

From the theoretical point of view, multiple ionization is a complex many-electron process to describe. In the case of ionization of He, sophisticated calculations have been developed that include correlation among electrons (the theoretical work on helium target is very extensive; see for example [26–32] and [15] and references therein). However, the extension to other targets is far from the present possibilities. For many-electron targets, the independent particle model (IPM) (multiple processes as a combination of single-electron ones, with no correlation) is the practical alternative.

On the other hand, direct ionization is not the only source of multiple ionization. There are different mechanisms of post-collisional ionization (PCI) that contribute to the finally measured charge state of the target, i.e. Auger and Coster–Kronig processes, electron shake-off, excitation followed by double Auger, among others. These processes were extensively studied by Carlson, Krause and co-workers [33–38] in photoionization. The advent of new experimental techniques in photon–atom research in the last two decades has contributed to a detailed knowledge of the Auger-type processes, the intermediate steps and cascades [39–53].

In the high-energy region (i.e. above 1 MeV), PCI is by far the most important contribution to multicharged target production, and it determines the ultimate experimental value. But the most interesting point is that PCI is time-delayed electron emission and can be considered independent of the projectile [5]. Probabilities of PCI are the same for proton, antiproton or electron impact. Moreover, they are the same in multiple ionization by photon impact.

Working within the IPM, Montenegro and collaborators [54, 55] and Kirchner and co-workers [56] proposed the inclusion of PCI in a semi-empirical way using experimental data of charge state distribution after single photoionization. This proposal boosted new experimental and theoretical research on this subject [57–69].

In the past few years, we have worked on the theoretical description of multiple ionization by positive-ion impact [66–69]. We obtained good results, mainly for protons in Kr and Xe. In the case of Ne, a systematic disagreement with the experimental data in the intermediate energy range was found. This discrepancy also appeared in the different approximations within the IPM (i.e. see Spranger *et al* [56], Galassi *et al* [62], Montanari *et al* [68]) introducing doubts about the limits of validity of the IPM and the importance of correlation among electrons.

The aim of this work is to advance in this research by comparing multiple-ionization cross sections by positive and negative charged-1 projectiles (protons, antiprotons and electrons). With this purpose, we present a detailed comparison of new theoretical calculations for antiproton and proton impact with available experimental data for proton, antiproton and also electron impact multiple ionization in the high-energy region. We find that this extended picture of the problem casts new light not only on previous doubts, but also on the discussion about the proton–antiproton–electron differences in terms of charge or mass effect, and in the inclusion of PCI in the total ionization cross sections.

We employ the CDW-EIS approximation to obtain the ionization probabilities as a function of the impact parameter for antiproton and proton impact. We have also included new first Born approximation results as a test in the high-energy region. The post-collisional electron emission is taken into account following [67]. Theoretical developments are introduced in section 2.

In section 3, we present, for the first time, a systematic comparison of the experimental single up to quintuple-ionization cross sections of Ne, Ar, Kr and Xe by antiproton, proton and electron impact in the energy range 25 keV to 10 MeV, together with CDW-EIS results for antiproton and proton impact, and first Born approximation up to 10 MeV (or 5.4 keV for electron impact energy). For very high energies, the first Born approximation can be extended to the description of electron impact multiple ionization under the assumption of straight line trajectory. In all the cases, the PCI contribution is included.

To our knowledge, present calculations are the first ones for multiple ionization including PCI by antiproton impact in such an extended energy range, and also for the heaviest rare gases. Some years ago, Kirchner and collaborators studied single, double and triple ionization by proton and antiproton impact on Ne [70] and Ar [71] using the non-perturbative basis generator method. This model proved to be very effective to describe these processes, but encountered certain intermediate energy discrepancies with antiproton measurements that will be discussed later on, in light of the more extended picture presented here.

Finally, the total ionization cross sections are calculated and compared with the experimental data, showing the importance of PCI even in the total ionization cross sections, which reaches 30% for Xe targets. These results are also included in section 3.

2. Theoretical model

2.1. CDW-EIS for proton and antiproton-impact ionization

The CDW-EIS, initially proposed by Crothers and McCann [72] and extended by Fainstein and co-workers [73, 74], is one of the most reliable approximations within the IPM to deal with calculations of ionization probabilities in the intermediate-to-high-energy regime [75–77]. Electron–electron correlation is totally excluded: the electrons ignore each other. Here we employ the CDW-EIS approximation to deal with proton and antiproton collisions.

In the case of antiproton impact ionization, previous calculations with the CDW-EIS were performed for total and differential cross sections of He [78–80]. For multiple ionization by proton impact, the CDW-EIS has already been employed by Rivarola and co-workers for multiple ionization of atomic and also molecular targets [62–64]. Recently, a study on multiple ionization of Ne, Ar, Kr and Xe for energies up to 1 MeV was presented by our group [67], including a detailed review on the photoionization branching ratios to include PCI.

In the present contribution, we improve our previous CDW-EIS calculations in [67] in two different senses. First, the maximum number of magnetic quantum numbers m was extended considerably to avoid aliasing (see the appendix for details). We found that the probability as a function of the impact parameter changes appreciably with the maximum value of m considered and with the accuracy of the integration. However, the integrated total value is very similar (the difference is 5% or 10% at most). Similar improvements were included in the first Born calculations. We obtained much more accurate ionization probabilities, and multiple-ionization cross sections of rare gases. In this sense, present proton impact ionization results replace those in [67].

Second, the calculations were performed up to 10 MeV and up to quintuple-ionization cross sections for all rare gases, from Ne up to Xe, which let us clarify the importance of PCI in the high-energy region.

2.2. Multiple ionization

Ionization probabilities as a function of the impact parameter are the first step in the multiple-ionization calculations. Within the IPM, the probability of direct ionization of exactly q_j electrons of the j sub-shell, $P_{(q_j)}(b)$, is obtained as a multinomial distribution of the ionization probabilities $p_j(b)$ as a function of the impact parameter b,

$$P_{(q_j)}(b) = \binom{N_j}{q_j} [p_j(b)]^{q_j}[1 - p_j(b)]^{N_j - q_j}, \tag{1}$$

where N_j is the total number of electrons in the sub-shell.

If a total of n target electrons are ionized from the different shells, $n = \sum_j q_j$, the total probability of direct ionization is

$$P_{(n)}(b) = \sum_{q_1+q_2+\cdots=n} \prod_j P_{(q_j)}(b) \tag{2}$$

and the cross section corresponding to the direct ionization of exactly n electrons is

$$\sigma_n = \int P_{(n)}(b)\ 2\pi\ b\ \mathrm{d}b. \tag{3}$$

The branching ratios of PCI, $F_{j,k}$, verify the unitary condition $1 = \sum_{k=0}^{k_{\max}} F_{j,k}$, with k being the number of electrons emitted in PCI after the single ionization of the $j = nlm$ sub-shell [67]. They are introduced in (1) following Montanari *et al* [67]:

$$P_{(q_j)}(b) = \binom{N_j}{q_j} \left[p_j(b) \sum_{k=0}^{k_{\max}} F_{j,k} \right]^{q_j} [1 - p_j(b)]^{N_j - q_j}. \tag{4}$$

Then, the addition of probabilities is rearranged in order to put together those terms that contribute to the same number of final emitted electrons, $q_j + k$. This rearrangement gives rise to new probabilities of exactly n emitted electrons including direct ionization and PCI, $P_{(n)}^{\mathrm{PCI}}$(see section 2.3 in [67] for details).

The multiple-ionization cross section of exactly n final emitted electrons, including direct ionization and PCI, is

$$\sigma_n^{\mathrm{PCI}} = \int P_{(n)}^{\mathrm{PCI}}(b)\ 2\pi\ b\ \mathrm{d}b, \tag{5}$$

with $P_{(n)}^{\mathrm{PCI}}(b)$ the probability of multiple ionization of exactly n electrons, including those emitted in direct ionization and those emitted due to PCI. As the method employed is unitarized, the following closure relations hold:

$$\sum_n P_{(n)}(b) = \sum_n P_{(n)}^{\mathrm{PCI}}(b) \tag{6}$$

and

$$\sum_n \sigma_n = \sum_n \sigma_n^{\mathrm{PCI}}. \tag{7}$$

In this work, the ionization probabilities $p_j(b)$ of the j sub-shell by proton and antiproton impact were calculated using the CDW-EIS approximation. We also obtained the corresponding values with the first Born approximation, which is still the most trustworthy and used model to describe the high-energy values. The convergence of the CDW-EIS to Born for impact energies above 1 MeV (or even less than 1 MeV in many cases) was tested. In fact, the extension of present calculations up to 10 MeV was done using the first Born approximation.

2.3. Total ionization

Total ionization cross sections have been much more studied, experimentally and theoretically, than multiple ionization. The largest volume of experimental data has been obtained for impact of electrons and protons, and reliable tabulations of data are available in the literature. We can mention for instance the works by Rapp and Englander-Golden [81] and Schram *et al* [21], with absolute measurements of the electron impact ionization cross sections for all rare gases, the compilations by Tawara and Kato [82] and by de Heer *et al* [19], and the review and suggested total cross sections by Rudd *et al* [83] in proton collisions.

When analysing ionization cross sections, there are two pairs of cross sections that must be clearly recognized and distinguished: gross and count cross sections [17, 19, 25, 84] on one hand, and exclusive and inclusive cross sections [85] on the other.

The so-called gross and count cross sections are related to the direct multiple-ionization cross sections σ_n of exactly n target electrons as follows:

$$\sigma_{\mathrm{gross}} = \sum_n n\ \sigma_n \tag{8}$$

and

$$\sigma_{\mathrm{count}} = \sum_n \sigma_n. \tag{9}$$

Physically, while σ_{gross} is a measure of total electron production, σ_{count} measures the production of positive ions. Gross cross sections are also known as the total or net ionization cross sections [25].

On the other hand, multiple-ionization cross sections σ_n of exactly n electrons emitted are also known as exclusive cross sections [85] and calculated within the IPM as in (3). Instead, the inclusive cross sections are related to the ionization of at least n electrons emitted, regardless of the final state of the remaining ones.

What is usually known in the literature as the total ionization cross section, σ_{Total}, and calculated as

$$\sigma_{\mathrm{Total}} = \sum_{\mathrm{nlm}} \sigma_{\mathrm{nlm}} \tag{10}$$

with $\sigma_{\rm nlm}$ the contribution of each *nlm* closed sub-shell,

$$\sigma_{\rm nlm} = 2 \int p_{\rm nlm}(b)\ 2\,\pi\ b\ {\rm d}b, \tag{11}$$

is the inclusive single-ionization cross section (ionization of at least one electron).

The general relationship between exclusive and inclusive cross sections is analytical and has been demonstrated by Sant'Anna *et al* [85]. In the case of the inclusive single-ionization cross section, $\sigma_{\rm Total}$ given by (10), it reads

$$\sum_{\rm nlm} \sigma_{\rm nlm} = \sum_{n} n\ \sigma_n \tag{12}$$

or

$$\sigma_{\rm Total} = \sigma_{\rm gross}. \tag{13}$$

The total cross section is an interesting magnitude. Theoretically, $\sigma_{\rm Total}$ can be worked out from each shell contribution, as in (10), without calculating the different multiple-ionization cross sections σ_n. Experimentally, electron flux can be measured without the knowledge of each multiple-ionization cross section. But the measurements do include PCI. When the total flux of electrons is measured, all the different ionization events are included, i.e. $\sigma^{\rm PCI}_{\rm Total}$ is measured instead of $\sigma_{\rm Total}$, with

$$\sigma^{\rm PCI}_{\rm Total} = \sum_{n} n\ \sigma^{\rm PCI}_{n}. \tag{14}$$

The analytical relationship given by (12) is valid for direct multiple ionization σ_n and not for final multiple-ionization cross sections including PCI, $\sigma^{\rm PCI}_n$. Even though count cross sections with or without PCI are the same (see (7)), gross cross sections are not equal with or without PCI:

$$\sum_{n} n\ \sigma_n \neq \sum_{n} n\ \sigma^{\rm PCI}_{n}, \tag{15}$$

and then

$$\sum_{\rm nlm} \sigma_{\rm nlm} \neq \sum_{n} n\ \sigma^{\rm PCI}_{n}. \tag{16}$$

In sum, $\sigma_{\rm count} = \sigma^{\rm PCI}_{\rm count}$, but $\sigma_{\rm Total} = \sigma_{\rm gross} < \sigma^{\rm PCI}_{\rm gross}$. We will analyse in section 3.2 the importance of PCI at the level of total ionization cross sections.

3. Results and discussions

3.1. Multiple-ionization cross sections

We present new theoretical results for multiple-ionization cross sections of Ne, Ar, Kr and Xe targets by impact of protons and antiprotons using CDW-EIS and the first Born approximation. In all cases studied, we tested the convergence of the CDW-EIS to Born for energies around 1 MeV or less (both, for direct ionization and for final ionization including PCI). For this reason, for energies above 1 MeV we continue the calculations straightforward with the first Born approximation.

The theoretical curves are compared with the experimental data available for antiprotons (p^-), protons (p^+) in the energy range (30 keV to 10 MeV), and also with experimental data of multiple ionization by electron (e^-) impact on equal velocity (electron energies up to 5.5 keV). In many cases, the e^- impact values represent the only experimental data to compare with, mainly for Kr and Xe in the high-energy region.

We include PCI contributions using the branching ratios, $F_{nl,k}$, of multiple ionization after single vacancy production measured in photoionization experiments. The values employed are those of table 1 in [67], which are the result of a review on the available photoionization data.

The empirical branching ratios include all possible PCI mechanisms, i.e. direct ionization followed by Auger, shake-off, cascades of complex processes. For valence shell electrons, Auger-like processes are not energetically allowed [35, 37, 43, 86]. In the present calculations, no PCI is included after single ionization of the outer shell. However, the role of a possible PCI due to shake-off will be discussed later in connection to double and triple ionization of Ne.

3.1.1. Single ionization. In figure 1, we present the theoretical single-ionization results for the Ne, Ar, Kr and Xe by p^+ and p^-, and the experimental data available in the literature. The curves of single ionization with PCI are on top of the direct ionization ones, except in the high-energy region where the inclusion of PCI reduces slightly the cross sections because part of the direct single ionization ends as multiple. The difference between direct results and those including PCI can be noted in Kr and Xe, but not in Ne and Ar even in the MeV region.

In general, the theoretical description agrees well with the experimental measurements. CDW-EIS results show differences between single-ionization cross sections by impact of p^+ and p^- around the maximum of the cross sections and in the low-energy region. Even in this energy region, the difference is clear for Ne, but is very small for Ar, Kr and Xe. The p^+ values are above the p^- ones near the maximum, and the opposite for lower energies. The same behaviour was found in single ionization of He by protons and antiprotons [17, 80]. We extend the CDW-EIS and the first Born calculations down to 25 keV to spy their behaviour below the maximum of the cross sections. By no means, we expect these approximations to be valid at such low-impact energies.

The comparison with the experimental data for p^- by Paludan *et al* [14] is very good for Kr and Xe, but for Ne and Ar certain disagreement is found at intermediate energies. Similar results are obtained by Kirchner *et al* [70, 71] in this energy region. It should be noted that these p^- cross sections were normalized to e^- single-ionization cross sections by Krishnakumar and Srivastava [24] above 500 keV, which perhaps explains the low values. For Ne and Ar below 800 keV, the separation between p^+ and e^- experimental data is important. In contrast, for Kr and Xe above 100 keV amu^{-1}, measurements for e^- and p^+ impact single-ionization cross sections agree quite well, and thus the normalization with this data is reasonable.

The p^+, p^-, e^- picture displayed in figure 1 shows that below certain impact energy, the experimental p^- cross sections are closer to p^+ ones (equal mass) than to e^- (equal charge). This behaviour will be noted in the different

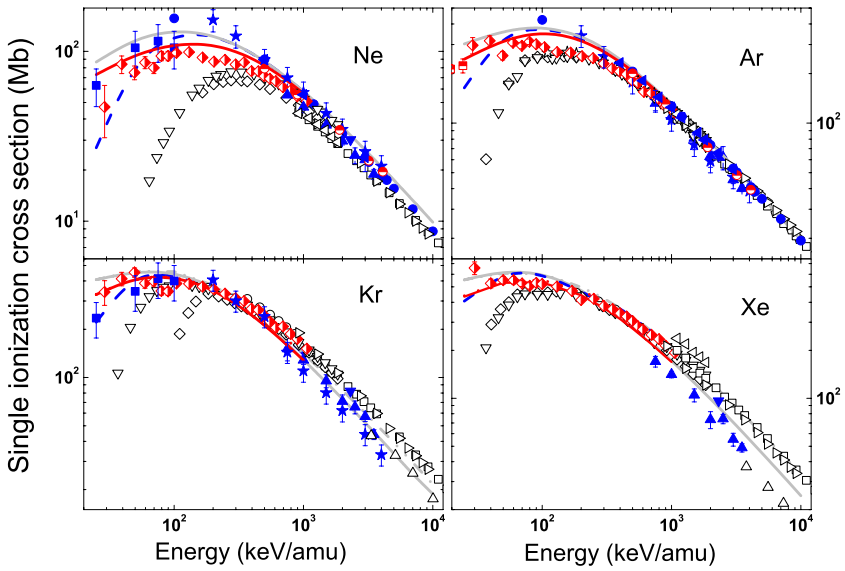

Figure 1. Single-ionization cross sections of Ne, Ar, Kr and Xe by proton, antiproton and electron impact. Curves: CDW-EIS results for antiprotons including PCI (red solid line) and direct ionization (red dotted line); CDW-EIS for protons including PCI (blue dashed line) and direct ionization (blue dashed-dotted line); Born results including PCI (grey solid line) and direct ionization (grey dashed-double-dotted line). Experimental data: for antiproton impact, Andersen *et al* [12], Paludan *et al* [14], Knudsen *et al* [15]; for proton impact, DuBois [1], DuBois *et al* [2], Andersen *et al* [12], Cavalcanti *et al* [55, 57], Gonzalez and Horsdal Pedersen [87], Haugen *et al* [88] at 2.31 MeV; and for electron impact, Schram *et al* [22], Krishnakumar *et al* [24], Nagy *et al* [25], Rejoub *et al* [89], Kobayashi *et al* [90], McCallion *et al* [91], Straub *et al* [92], El–Sherbini *et al* [93]. The nomenclature is in figure 2.

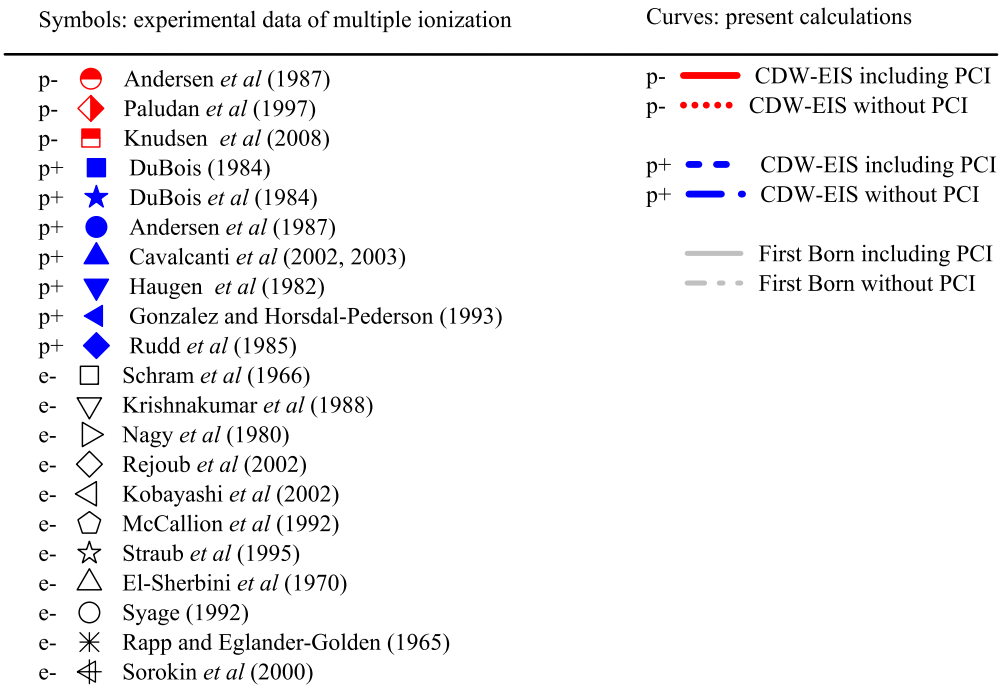

Figure 2. Nomenclature used in figures 1, 3, 4, 5, 6, 7, 8, 9, 10 and 11.

multiple-ionization cross sections showing that in the low and intermediate energy region mass effect may prevail over charge effect in the dynamics of the collision.

In figure 1, we also include the data by Andersen *et al* [12] for p^- in Ne and Ar, and by Knudsen *et al* [15] for p^- in Ar (only one value included at 25 keV). The measurements for low-impact energies in [15] match well with the previous ones by Paludan *et al* [14] at higher energies.

The data for p^+ impact in Ne, Ar and Kr by DuBois *et al* [2] include capture. For this reason in figure 1, we only display the measurements for $E \geqslant 200$ keV, where capture contribution is expected to be negligible. The first measurements using coincidence technique to separate capture and pure ionization channels in multiple ionization were performed by DuBois [1] in 1984 for multiple ionization of Ne and Kr by p^+ at impact energies $E \leqslant 100$ keV. The

importance of separating capture from ionization is clear in these experimental values. The data by DuBois [1] have also been included in figure 1. We do not expect the CDW-EIS to be valid for impact energies below 70 or 50 keV; within this limit, the agreement with the measurements in [1] is reasonable.

For p^+ impact in Ne and Ar, the agreement among the experimental data by Andersen *et al* [12], Dubois *et al* [2], Cavalcanti *et al* [55, 57] and Haugen *et al* [88], and the theoretical description is good.

The values displayed in figure 1 for p^+ and p^- on Ne and Ar by Andersen *et al* [12], for p^+ on Ne and Ar by Gonzalez and Horsdal Pedersen [87] and for p^+ in the four targets by Haugen *et al* [88] were obtained from the measured relative double to single, $R_{21} = \sigma_2/\sigma_1$, and triple to single, $R_{31} = \sigma_3/\sigma_1$, and normalized to the recommended values for total ionization cross sections in p^+ collisions by Rudd *et al* [83] as follows:

$$\sigma_1 = \frac{\sigma_{\text{Total}}^{\text{Rudd}}}{(1 + 2R_{21} + 3R_{31})}. \tag{17}$$

Double- and triple-ionization cross sections σ_2 and σ_3 were obtained directly using the results of (17). In the case of p^-, we only normalized to Rudd values for energies above 500 keV amu^{-1} (high energies for which p^+ and p^- values converge).

Multiple-ionization data by e^- deserve separate comments. Among the available e^- data for multiple ionization, there are absolute measurements like those by Rejoub *et al* [89], Nagy *et al* [25], Schram *et al* [21–23] and Straub *et al* [92]. Instead, the data by Krishnakumar *et al* [24] and by McCallion *et al* [91] were normalized to the total ionization cross sections by Rapp and Englander-Golden [81], and the results by Kobayashi [90] were normalized to the total cross sections by Schram *et al* [21].

In the high-energy region, the CDW-EIS results for Ne are rather good, but are 10% above the data by Andersen *et al* [12] above 5 MeV. In the case of the Ar target, at high energies our calculations agree very well with the experimental data, not only for p^+ but also for e^- impact. In this target, e^- and p^+ data follow the same trend. For Kr and Xe, a great dispersion among experimental data can be observed. Present theoretical results are in between them.

For e^- in Ne, the measurements by Adamczyk *et al* [23] are very close to previous results by the same group of Schram and collaborators [22], and were not included for clarity of the figure.

3.1.2. Double ionization. Our theoretical results for double ionization of Ne, Ar, Kr and Xe by p^+ and p^- are displayed in figure 3, together with the experimental data available. In the case of e^- impact, we include the measurements above the maximum of the cross sections, which for double ionization implies higher energies than for single ionization.

Again, the theoretical results for direct ionization may be hidden by final values including PCI when both coincide. This is the case of Ne and Ar for impact energies $E < 1$ MeV, while for Kr (Xe) the curves clearly separate each other at 500 keV (300 keV).

The comparison shows in general a good approximation to the picture of the double ionization, with the importance of PCI being very clear in all the cases.

About the experimental data, again we include the results by DuBois [1] for p^+ impact in Ne and Kr at energies below 100 keV amu^{-1}, and the data by DuBois *et al* [2] for energies above 200 keV. The agreement between our CDW-EIS results for Ne and Kr and the data for low energies shows the correct trend of the theory in this energy region.

The p^- data by Paludan *et al* [14] are correctly described for double ionization of Ar and Xe in the whole energy range. For Ne and Kr there is a region above 300 keV amu^{-1} for Kr (and 600 keV amu^{-1} for Ne) where the experimental data for p^- seem to be high as compared with p^+ and e^- experimental results and with the CDW-EIS.

At this stage, it is important to note that *e–e* correlation is completely excluded within the IPM: the electrons ignore each other. In the high-energy limit, it tends to the first Born approximation (q^2 dependence, no difference between p^+ and p^-). In the case of He target, the double to single-ionization ratio for p^- is a factor of 2 as compared with the same ratio for p^+ even at 2 MeV [10]. This charge effect has been adjudicated to the interference of amplitudes leading to a term proportional to q^3 [10] (the two step two (TS-2) processes, related to the interaction of the projectile with two electrons; and the two step one (TS-1) process, in which the projectile ionizes one electron and the *e–e* interaction causes the emission of the second electron).

In the cases displayed in figure 3, our CDW-EIS double-ionization cross sections for p^- and p^+ are very close for impact energies above 200 or 300 keV amu^{-1}, depending on the target. In some cases, p^+ data are better described than p^- (i.e. Kr), in others it is just the opposite (i.e. Ar). In view of the four rare gases studied here, our theory does not help us to fully understand the experimental p^+–p^- difference in that energy region.

The inclusion of e^--impact data emphasizes the high-energy behaviour for all the targets. This high-energy region dominated by the PCI contributions is well described for Kr and Xe, or even for Ar, but is clearly underestimated for Ne.

For Ar, our theory with PCI is somewhat low above 3 MeV. The experimental data for e^-, p^+ and p^- agree quite well with each other. The data by Dubois for p^+ in Ar seem to be low as compared with the rest.

For double ionization of Ar by e^- impact, also known as the (e,3e) process, a theoretical description including PCI was proposed by Jha *et al* [95]. These authors considered that the 100% of the single ionization of the 2p-electrons of Ar ends as double ionization. Instead, our calculations use the experimental yields of PCI by Brunken *et al* [46] and by Viefhaus *et al* [47] that agree in that 87% of the single ionization of the 2p sub-shell ends up as double ionization and 13% as triple ionization.

The case of Ne is different from the others. In the high-energy region the major group of experimental data is underestimated by the theory, showing that PCI is not well described in this case.

In Ne only the K-shell contributes to PCI. As in the other targets, we did not include PCI after direct ionization

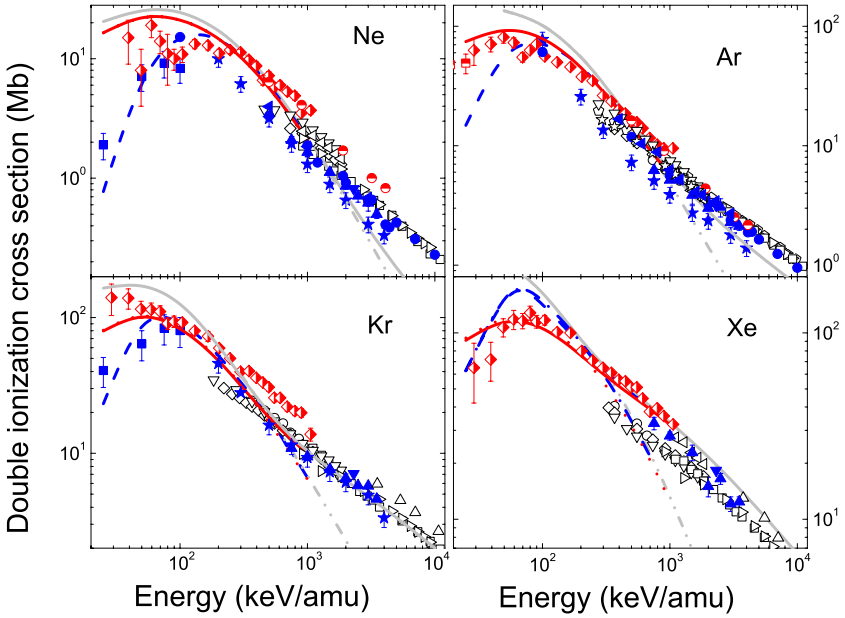

Figure 3. Double-ionization cross sections of Ne, Ar, Kr and Xe by proton, antiproton and electron impact. Curves as in figure 1. Experimental data: for antiproton impact, Andersen *et al* [12], Paludan *et al* [14], Knudsen *et al* [15]; for proton impact, DuBois [1], DuBois *et al* [2], Andersen *et al* [12], Cavalcanti *et al* [55, 57], Gonzalez and Horsdal Pedersen [87], Haugen *et al* [88] at 2.31 MeV; and for electron impact, Schram *et al* [22], Krishnakumar *et al* [24], Nagy *et al* [25], Rejoub *et al* [89], Kobayashi *et al* [90], McCallion *et al* [91], Straub *et al* [92] El-Sherbini *et al* [93] and Syage [94]. The nomenclature is in figure 2.

of a valence electron. As far as we know, there is no direct experimental evidence of PCI after the 2s and 2p single ionization of Ne. However, the results displayed in figure 3 may be an indirect proof of this contribution.

Auger processes are the main mechanism of PCI of inner-shells, but they are not energetically possible for the outer-shell. An interesting mechanism of direct ionization followed by PCI is shake-off. The change in the potential gives an overlap of wavefunctions and a probability to excite other electrons into the continuum (electron shake-off) or into discrete excited states (electron shake-up) [96]. This mechanism has been theoretically studied by different groups since the work by Carlson and Nestor [96, 97] and Mukoyama and co-workers [98, 99] to date [100, 101].

The theoretical calculations by Carlson and Nestor [96] and Mukoyama *et al* [99] for Ne agree in a shake probability (shake up plus shake-off) of 0.045 and 0.043 for 2s and 2p initial vacancy, respectively, and they argue about equipartition between excitation and ionization for initial outer-shell ionization [96]. This is, as a first approximation, a shake-off probability around 0.02, equal for 2s or 2p initial vacancy.

The inclusion of shake-off following these theoretical calculations enhances the cross sections in the whole energy range (not only in the high-energy region) because it is PCI related to outer-shell ionization. The results of our present CDW-EIS and first Born calculations for p^+ and p^- in Ne, including PCI of inner-shells (experimental branching ratios) and theoretical shake-off of the valence shell, are displayed in figure 4. These values were obtained using the branching ratios of table 1 in [67], but changing those of 2s and 2p vacancy from $F_{2s,0} = F_{2p,0} = 1$ and $F_{2s,1} = F_{2p,1} = 0$ (no PCI of these sub-shells) to $F_{2s,0} = F_{2p,0} = 0.98$ and $F_{2s,1} = F_{2p,1} = 0.02$,

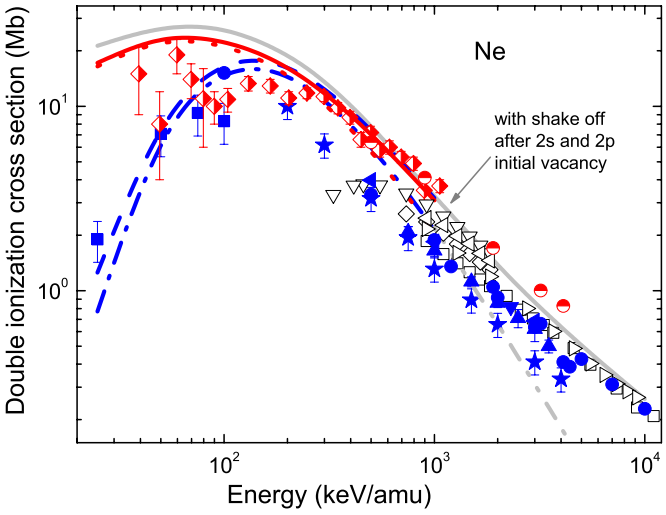

Figure 4. Double-ionization cross sections including PCI of the K-shell and shake-off of the 2s and 2p electrons considering that 2% of the single ionization of these sub-shells end up as double ionization (see the comment in the text). Curves and symbols as in figure 3.

considering the shake-off calculations by Carlson and Nestor [96] and Mukoyama *et al* [99].

The main difference between this calculation and previous ones [56, 62, 67, 68] is the inclusion of PCI from the 2s and 2p sub-shells of Ne due to shake-off. Note that the branching ratios employed for the rest of the sub-shells (inner ones) are experimental values that include all contributions to PCI (Auger, shake-off or different cascades and combination of processes).

The change in the theoretical results shows the correct trend at high energies. The enhanced values in the whole energy range also improved the comparison with the p^+ data at low energies [1] and with the p^- data at intermediate energies [14].

In this work, we include shake off following single ionization of the L-shell of Ne. There is no reason to consider this outer-shell contribution only in Ne and not in the other targets. But it is reasonable to think that in the case of Ne it could be more important than in Ar, Kr or Xe, because in Ne only the K-shell contributes to PCI. In the other atoms, many subshells are taken into account, and this may mask to some extent the effect. The PCI following ionization of valence electrons should be studied to a greater extent in the future.

The case of Ne is different from the others in another aspect: the overestimation of p^+ data in the intermediate energy region (i.e. for impact energies 0.5–1 MeV, the data by Dubois *et al* [2], Andersen *et al* [12] and Gonzalez *et al* [87] are a factor 2 below the CDW-EIS results). This case was presented in the introduction as one of the theoretical–experimental disagreements that motivate this work. Similar theoretical overestimation of p^+ data below 1 MeV has already been noted by Spranger and Kirchner [56], and it has been considered as a possible limiting factor of the IPM [56, 67]. The results displayed in figure 4 give a different perspective to this discussion due to the comparison with the p^- data. We can say that the IPM (in the present case, the CDW-EIS) describes rather well the experimental values for double ionization of Ne by p^- at intermediate energies (i.e. 0.2–2 MeV), but is not so good for p^+ impact at the same energies. There is a clear difference between p^- and p^+ data below 1 MeV, which does not appear in the theoretical description.

3.1.3. Triple ionization. In figure 5, we present our results for triple-ionization cross sections. The theoretical curves including PCI show a very good description of the experimental data for Ar above 400 keV and for Kr and Xe in the whole energy range, including the data of p^- for (30–1000) keV.

For Ne and Ar, the situation is more revealing. The theory presents a pronounced difference between p^+ and p^- impacts around the maximum of the cross sections, greater than for double or single ionization. For Ar targets, the experiments do not seem to be sensitive to this change. But for Ne, this difference is very remarkable. At the same time, there is a large spread among experiments which casts some doubts.

Again the high-energy data for Ne is underestimated, opening the discussion about the PCI of valence electrons also in Ne^{3+} production. A very good agreement would be obtained for double- and triple-ionization cross sections if the 2% of shake-off from 2s and 2p sub-shells is split into 1.9% to double and 0.1% to triple ionization. This proves the shake-off calculation to be an interesting subject for future work.

About the e^- impact data, it is interesting to note that they allow us to extend the theoretical–experimental comparison for Kr and Xe for impact energies in the range (4–10) MeV (electron energy above 2 keV), where no p^+ or p^- data are available.

The first Born calculations including PCI describe very well the e^--impact triple-ionization cross sections for Ar, Kr and Xe for electron energies above 500 eV.

3.1.4. Quadruple ionization. Figure 6 shows a poorer experimental scenario due to the lack of measurements of quadruple ionization by p^-. Moreover, for Ne only e^--impact data are available in the literature.

The separation between direct ionization and total ionization including PCI is very clear in the four targets, being more than one order of magnitude for Ar, Kr and Xe.

The theoretical description is quite good, especially with the data for p^+ in Kr by DuBois [2], which covers an extended energy range.

In the case of Xe, a clear theoretical underestimation of the experimental values above 2 MeV is observed. The extended picture up to 10 MeV and the comparison with electron impact data shows the agreement between p^+ measurements by Cavalcanti *et al* [57] and e^- ones by Schram [22], Kobayashi *et al* [90] and Rejoub *et al* [89]. The e^- values by Krishnakumar and Srivastava [24] are about twice those reported by Schram *et al* [22] as already noted by these authors.

The theoretical underestimation of Xe quadruple ionization is probably due to PCI following ionization of deep shells, not included in our present calculations. For Ne and Ar, we include all the shells in the calculation (K and L, or K, L and M-shell, respectively). In the case of Kr and Xe, only the two outer shells have been considered (M and N-shells for Kr and N and O-shells for Xe). This limitation may have effects in the quadruple- and quintuple-ionization cross sections.

3.1.5. Quintuple ionization. The quintuple-ionization cross sections show clearly the lack of experimental data already mentioned, as can be observed in figure 7. For Ne and Ar, only e^--impact data are available. The comparison of present calculations with these measurements shows that the Born approximation with PCI gives a good high-energy description of e^--impact quintuple ionization, mainly for Ar.

For Kr and Xe, there are two sets of p^+ data, by DuBois *et al* [2] and by Cavalcanti *et al* [57], respectively. The agreement between theoretical curves and p^+ data is reasonable.

The e^--impact measurements for quintuple ionization of Kr and Xe indicate a certain underestimation of the data for energies $E > 5$ MeV for Kr (i.e. electron impact energy $E_e > 2.5$ keV) and for $E > 2$ MeV for Xe (i.e. $E_e > 1$ keV). Again, the inclusion of PCI after ionization of very deep shells may correct this problem.

3.2. Total ionization cross sections

We compare experimental total ionization cross sections with our total cross sections including PCI, $\sigma_{\text{Total}}^{\text{PCI}}$, as calculated in (14). To make a detailed comparison, in table 1 we include the proton and antiproton impact theoretical total or gross cross sections for direct ionization defined in (8), the total ionization cross sections including PCI, given by (14), and the count cross sections, which are equal with or without PCI (see (7) and (9)).

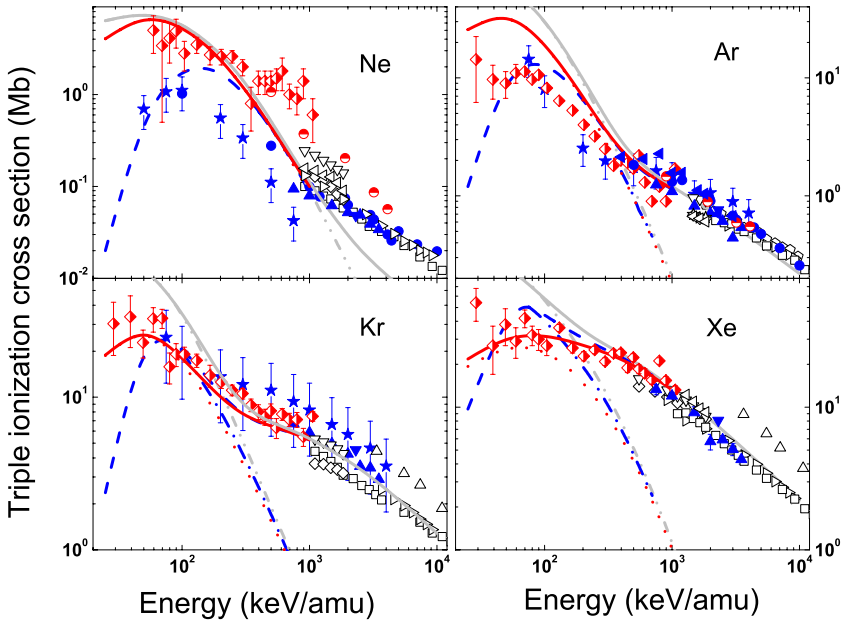

Figure 5. Triple-ionization cross sections of Ne, Ar, Kr and Xe by proton, antiproton and electron impact. Curves as in figure 1. Experimental data: for antiproton impact, Andersen *et al* [12], Paludan *et al* [14]; for proton impact, DuBois *et al* [2], Andersen *et al* [12], Cavalcanti *et al* [55, 57], Gonzalez and Horsdal Pedersen [87], Haugen *et al* [88] at 2.31 MeV; and for electron impact, Schram *et al* [22], Krishnakumar *et al* [24], Nagy *et al* [25], Rejoub *et al* [89], Kobayashi *et al* [90], McCallion *et al* [91], Straub *et al* [92], El–Sherbini *et al* [93] and Syage [94]. The nomenclature is in figure 2.

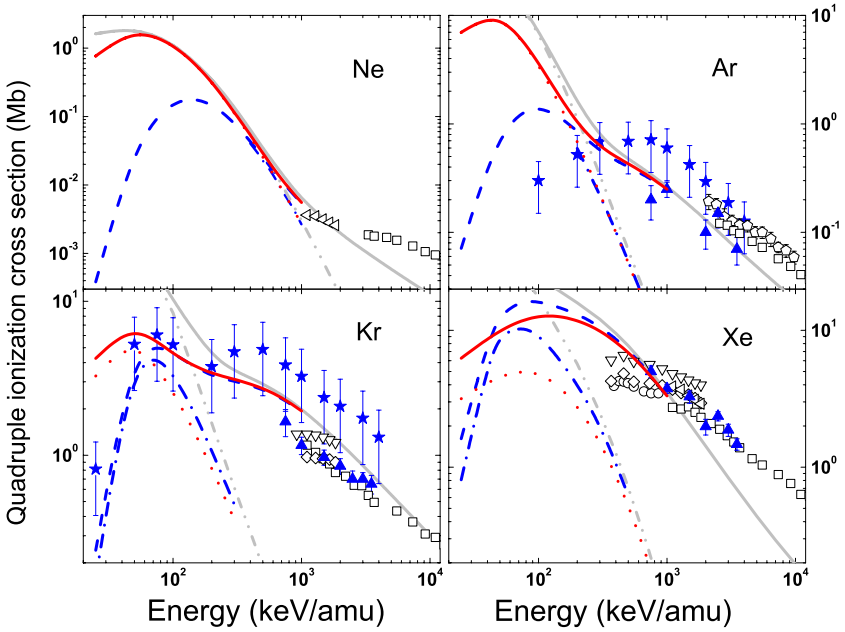

Figure 6. Quadruple-ionization cross sections of Ne, Ar, Kr and Xe by proton, antiproton and electron impact. Curves as in figure 1. Experimental data: for proton impact, DuBois *et al* [2], Cavalcanti *et al* [57] and for electron impact, Schram *et al* [22], Krishnakumar *et al* [24], Rejoub *et al* [89], Kobayashi *et al* [90], McCallion *et al* [91], Straub *et al* [92], Syage [94]. The nomenclature is in figure 2.

In the seventh column of this table, we include the ratio between gross cross sections with and without PCI:

$$\frac{\sum n\,\sigma_n^{\mathrm{PCI}}}{\sum n\,\sigma_n}. \tag{18}$$

This value is a measure of the importance of PCI in the total ionization cross section.

In the last column of table 1, we display the ratio of gross cross section with PCI and count cross section

$$\langle n\rangle = \sum n\,\sigma_n^{\mathrm{PCI}} \Big/ \sum \sigma_n = \sum n\,\sigma_n^{\mathrm{PCI}} \Big/ \sum \sigma_n^{\mathrm{PCI}}. \tag{19}$$

This ratio $\langle n\rangle$ is also known as the mean number of emitted electrons or the average recoil ion charge [69].

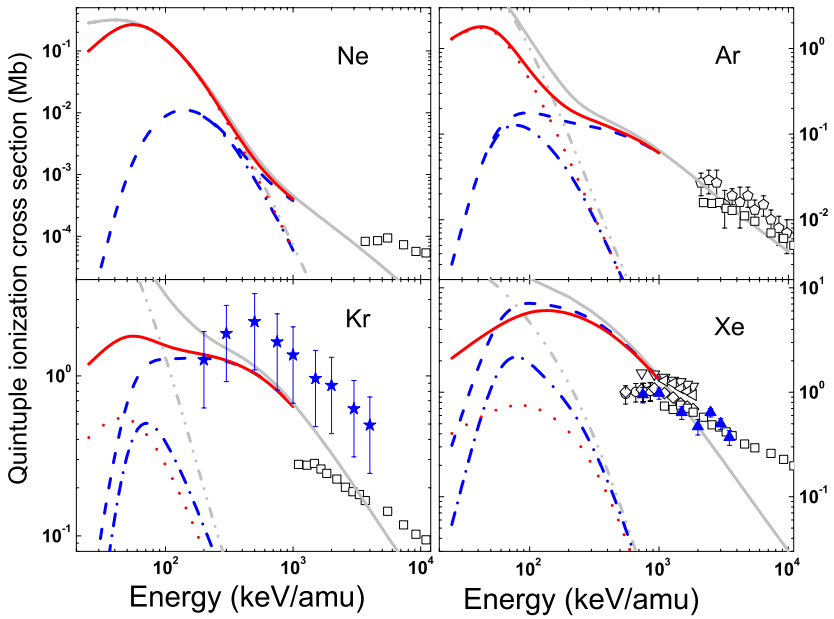

Figure 7. Quintuple-ionization cross sections of Ne, Ar, Kr and Xe by proton, antiproton and electron impact. Curves as in figure 1. Experimental data: for proton impact, DuBois *et al* [2] and Cavalcanti *et al* [57], and for electron impact, Schram *et al* [22], Krishnakumar *et al* [24], Rejoub *et al* [89], Kobayashi *et al* [90], McCallion *et al* [91], Straub *et al* [92] and Syage [94]. The nomenclature is in figure 2.

Table 1. CDW-EIS gross and count cross sections for antiproton and proton impact on rare gases in units of 10^{-16} cm^2. The ratio of gross cross sections with and without PCI, and the values for $\langle n\rangle = \sum n\,\sigma_n^{\rm PCI}/\sum\sigma_n$ (ratio between gross cross sections with PCI and count cross sections) are also included. The results for $E = 1,\ 2$ and 10 MeV were obtained with the first Born approximation. The convergence of CDW-EIS to Born values at these energies was previously checked.

Target	E (MeV)		$\sum n\,\sigma_n$	$\sum n\,\sigma_n^{\rm PCI}$	$\sum\sigma_n$	$\frac{\sum n\,\sigma_n^{\rm PCI}}{\sum n\,\sigma_n}$	$\frac{\sum n\,\sigma_n^{\rm PCI}}{\sum\sigma_n}$
Ne	0.2	p^+	1.56	1.56	1.38	1.00	1.13
	0.2	p^-	1.46	1.46	1.25	1.00	1.17
	0.4	p^+	1.15	1.15	1.06	1.00	1.08
	0.4	p^-	1.08	1.08	9.87(−1)	1.00	1.09
	1	Born	6.29(−1)	6.29(−1)	6.04(−1)	1.00	1.04
	2	Born	3.71(−1)	3.72(−1)	3.64(−1)	1.00	1.02
	10	Born	9.97(−2)	1.00(−1)	9.94(−2)	1.00	1.01
Ar	0.2	p^+	4.39	4.41	3.79	1.00	1.16
	0.2	p^-	4.30	4.31	3.69	1.00	1.17
	0.4	p^+	2.84	2.87	2.61	1.01	1.10
	0.4	p^-	2.80	2.84	2.57	1.01	1.10
	1	Born	1.44	1.49	1.39	1.03	1.07
	2	Born	8.17(−1)	8.50(−1)	8.02(−1)	1.04	1.06
	10	Born	2.06(−1)	2.16(−1)	2.04(−1)	1.05	1.06
Kr	0.2	p^+	4.97	5.10	4.22	1.03	1.20
	0.2	p^-	4.77	4.94	4.11	1.04	1.20
	0.4	p^+	3.11	3.31	2.81	1.06	1.18
	0.4	p^-	3.06	3.28	2.79	1.07	1.18
	1	Born	1.56	1.78	1.49	1.14	1.19
	2	Born	8.82(−1)	1.05	8.57(−1)	1.19	1.22
	10	Born	2.19(−1)	2.74(−1)	2.17(−1)	1.25	1.26
Xe	0.2	p^+	7.62	8.21	6.16	1.08	1.33
	0.2	p^-	6.85	7.51	5.68	1.10	1.32
	0.4	p^+	4.78	5.53	4.16	1.16	1.33
	0.4	p^-	4.58	5.34	4.02	1.17	1.33
	1	Born	2.40	3.00	2.24	1.25	1.34
	2	Born	1.36	1.75	1.31	1.29	1.34
	10	Born	3.37(−1)	4.51(−1)	3.34(−1)	1.34	1.35

Table 1 summarizes some of the most interesting results of the present contribution. Note that the values displayed in column 4 are the usual theoretical total ionization cross section calculated by adding contributions from each sub-shell, as in (10). However, experimental ionization cross sections include PCI, not only in each multiple cross section (as displayed

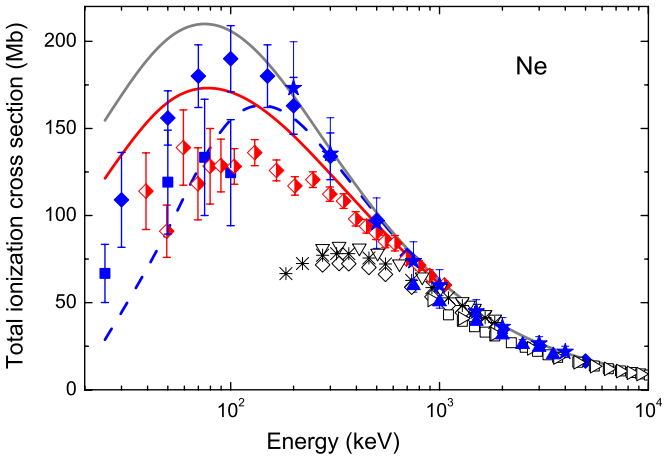

Figure 8. Total ionization cross section of Ne by proton, antiproton and electron impact. Curves, CDW-EIS results for antiprotons (red solid line) and protons (blue dashed line); Born results, grey solid line. Note that theoretical curves are $\sigma_{\text{Total}}^{\text{PCI}}$ given by (14). Experimental data: for antiproton impact, Paludan *et al* [14]; for proton impact, DuBois [1], DuBois *et al* [2], Cavalcanti *et al* [55], Rudd *et al* [83]; and for electron impact, Schram *et al* [21], Krishnakumar *et al* [24], Nagy *et al* [25], Rejoub *et al* [89], Rapp and Eglander-Golden [81]. Symbols are given in figure 2.

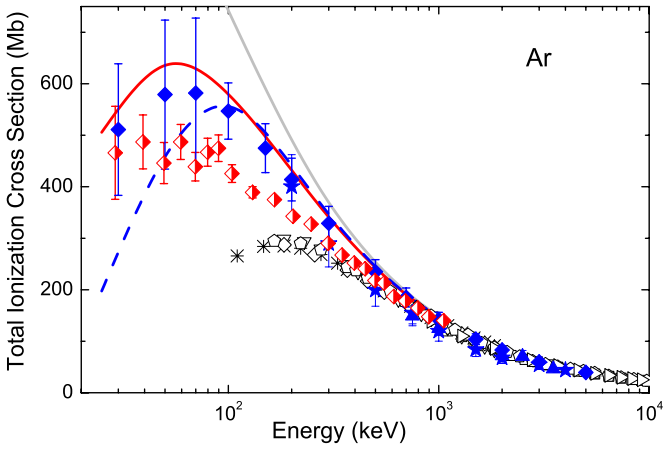

Figure 9. Total ionization cross section of Ar by proton, antiproton and electron impact. Curves, as in figure 8. Experimental data: for antiproton impact, Paludan *et al* [14]; for proton impact, DuBois *et al* [2], Cavalcanti *et al* [57], Rudd *et al* [83]; and for electron impact, Schram *et al* [21], Krishnakumar *et al* [24], Nagy *et al* [25], Rejoub *et al* [89], McCallion *et al* [91], Rapp and Eglander-Golden [81]. Symbols are given in figure 2.

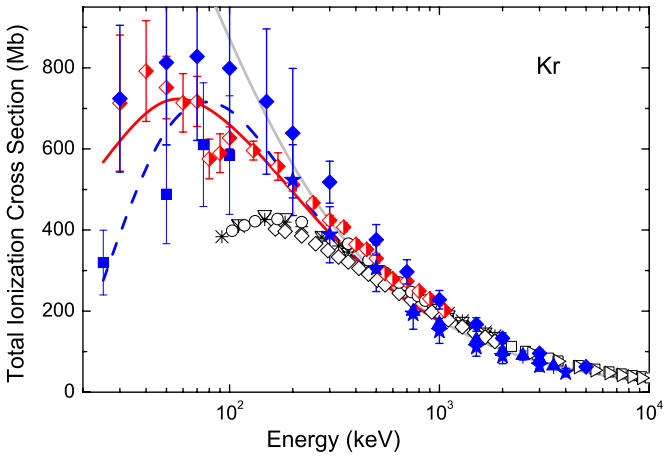

Figure 10. Total ionization cross section of Kr by proton, antiproton and electron impact. Curves as in figure 8. Experimental data: for antiproton impact, Paludan *et al* [14]; for proton impact, DuBois [1], DuBois *et al* [2], Cavalcanti *et al* [57], Rudd *et al* [83]; and for electron impact, Schram *et al* [21], Krishnakumar *et al* [24], Nagy *et al* [25], Rejoub *et al* [89], Syage [94], Rapp and Eglander-Golden [81]. Symbols are given in figure 2.

in the previous section), but also in the total cross sections as well. This means that we have to add PCI contributions even to total ionization cross sections, and that the calculated $\sigma_{\text{total}} = \sum_{\text{nlm}} \sigma_{\text{nlm}}$ are not the finally measured ones. As we can observe in the ratios displayed in column 7 of table 1, the difference obtained in the total cross sections by including PCI is negligible for Ne and even for Ar up to 10 MeV. However, its importance increases with the target atomic number, being around 20% for Kr and 30% for Xe for impact energies above 1 MeV.

The ratios between the theoretical gross and count cross sections in column 8 of table 1 are in good agreement with recommended values for e^- impact ionization [19].

Most of the theoretical and experimental work on total ionization cross sections found in the literature are gross cross sections. However, the very accurate measurements of electron-impact ionization cross sections by Sorokin *et al* [84] are actually count cross sections. The e^- impact total ionization cross sections for the four rare gases calculated by Bartlett and Stelbovics [102], and the recent semi-empirical ones by Naghma *et al* [103] are compared with the experimental count cross sections by Sorokin *et al* [84]. This comparison is not correct for heavy elements.

In figures 8, 9, 10 and 11, we display our CDW-EIS and the first Born approximation results for $\sigma_{\text{Total}}^{\text{PCI}} = \sum n\,\sigma_n^{\text{PCI}}$ together with the experimental data available. These experimental values have been measured directly as total ionization cross sections, $\sigma_{\text{Total}}^{\text{exp}}$ [21, 81, 83], or they have been obtained from the experimental multiple-ionization cross section as $\sigma_{\text{Total}}^{\text{exp}} = \sum n\,\sigma_n^{\text{exp}}$ from [1, 2, 14, 24, 25, 55, 57, 89, 91, 94].

In all these figures, we include the total cross sections for p^+, p^- and also the experimental data for e^- impact at high energies. Above 800 keV, the CDW-EIS values for p^+ and p^- clearly converge to Born ones. In this high-energy region also the experimental data for p^+, p^- and e^- follow the same trend, and the theoretical–experimental agreement is good.

For p^+ impact ionization, we include in figures 8, 9, 10 and 11 the recommended values by Rudd *et al* [83]. These values fit a large number of experimental data since Gilbody and Hasted [104] in 1957 up to Rudd *et al* in 1983 [105] (see [83] and references therein).

In the case of Ne displayed in figure 8, for energies around 100 keV, the p^+–p^- theoretical difference is clear. The p^+ results are above p^- results for energies just above the maximum, probably a sequel of the so-called Barkas effect, but are below p^- results for lower energies. Similar behaviour has been obtained for ionization of He (see, for example, the reviews [10, 17] and references therein [80, 15]).

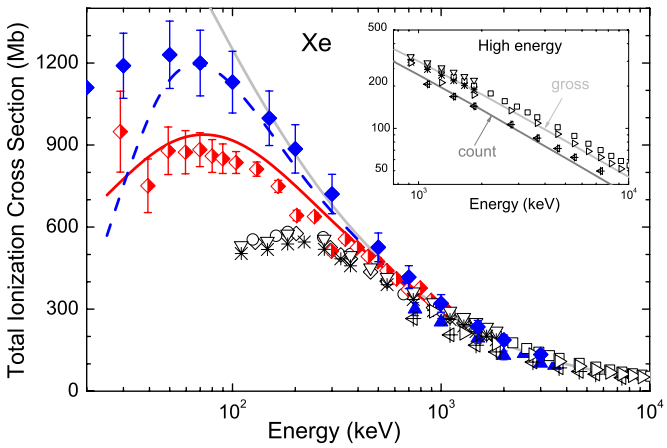

Figure 11. Total ionization cross section of Xe by proton, antiproton and electron impact. Curves as in figure 8. In the inset, the high-energy plot showing the difference between $\sigma_{\rm gross}$ and $\sigma_{c}ount$. Experimental data: for antiproton impact, Paludan *et al* [14]; for proton impact, Cavalcanti *et al* [57], Rudd *et al* [83]; and for electron impact, Schram *et al* [21], Krishnakumar *et al* [24], Nagy *et al* [25], Rejoub *et al* [89], Syage [94], Rapp and Eglander-Golden [81] and Sorokin *et al* [84]. Symbols are given in figure 2.

Note in figures 8 and 10 that while the total values for p^+ suggested by Rudd *et al* [83] may include capture at energies below 150 keV, the measurements by DuBois [1] for energies below 100 keV explicitly exclude capture processes.

The experimental values for ionization by e^- impact by Krishnakumar *et al* [24] are normalized to Rapp and Englander-Golden [81] only for single ionization. Total cross sections are not equal, but very similar.

For Ar, the theoretical total ionization cross sections for p^+ and p^- are very similar for impact energies above 120 keV, as observed in figure 9. However, p^- experimental cross sections are below the theoretical expectations. On the other hand, our CDW-EIS values for p^- impact energies above 50 keV are very close to those by Kirchner *et al* [71], using the time-dependent solution of the Schrödinger equation with the basis generator method (TDSE-BGM).

In the case of Kr in figure 10, the agreement with p^- experimental data by Paludan *et al* [14] and with p^+ values measured by DuBois, Toburen and Rudd [2] above 200 keV is good. The agreement with the recommended total cross sections by Rudd *et al* [83] above 50 keV is good, considering that the uncertainty of these values is large.

Finally, the results for total ionization cross sections of Xe displayed in figure 11 are in very good agreement with p^+ and p^- experimental data for impact energies above 50 keV. Above 4 MeV, the theoretical–experimental comparison is possible due to e^- impact measurements at high velocities. To our knowledge no p^+ or p^- data are available. We have included in this figure the experimental cross sections by Sorokin *et al* [84], which are clearly count cross sections. These values are 30% below the theoretical gross cross sections including PCI, as expected from table 1.

We followed Bartlett and Stelbovits [102] in emphasizing the high-energy behaviour to note the difference between one group of experimental data of total or gross cross sections [21, 24, 25, 81], and the other of count cross sections [84]. To illustrate this point in figure 11, we include as an inset the high-energy plot in the logarithmic scale. In this inset, we include the first Born results for both total cross sections including PCI (gross) and count cross sections. The experimental data by Schram *et al* [21], Nagy *et al* [25], Krishnakumar *et al* [24] and Rapp *et al* [81] are very well described by the first Born gross cross sections. On the other hand, the theoretical count cross sections show good agreement with the corresponding experimental data by Sorokin *et al* [84]. Therefore, at high energies the simple first Born approximation accounts very well for both gross and count cross sections. In fact, count cross sections appear as an interesting value for the theoretical–experimental comparison as they do not depend on PCI.

4. Conclusions

We have presented new theoretical results for multiple ionization by proton, antiproton and electron impact on the four rare gases. The calculations were performed using the CDW-EIS and also with the first Born approximation, covering an extended energy range, from 50 keV up to 10 MeV.

We have found that this extended picture of the problem shows that IPM works reasonably well for antiproton impact even in the intermediate energy region. Also of interest in this comparison is the discussion about the proton–antiproton–electron differences in terms of charge or mass effect. Total ionization cross sections have also been calculated, and the importance of PCI even in total cross sections has been studied. Our calculations show that this difference is very small for Ne or Ar but increases with the target atomic number, being 30% for Xe at high energies.

Some points need further study: Ne proved to be the most complicated target to be described, the proton–antiproton difference just below 1 MeV, or the effect of possible shake-off of valence electrons, which should be scrutinized in the future, including a study of its possible influence also for the other atoms. On the other hand, for the heavier rare gases, the influence of the deep shells (L and M-shells for Kr and Xe, respectively) seems to be decisive for multi-charged ion production in the high-velocity regime and needs to be calculated. Our present efforts aim in these directions.

Acknowledgments

This work was partially supported by the Argentinean CONICET, the Agencia Nacional de Promoción Científica y Tecnológica and the Universidad de Buenos Aires.

Appendix. Impact parameter calculation

We found it convenient to expand the T-matrix element for a given angle (Ω), energy (E) of the ejected electron and momentum transfer ($\vec{\eta} = \{\eta, \varphi_\eta\}$) as follows:

$$T(E, \Omega, \eta, \varphi_\eta) = \sum_{m=-l_{\max}}^{l_{\max}} i^m \frac{\exp(im\,\varphi_\eta)}{\sqrt{2\pi}} T_m(E, \Omega, \eta), \quad \text{(A.1)}$$

where $l_{\max}$ is the maximum orbital momentum used. The probability of transition $P(E, \Omega, \vec{b})$ as a function of

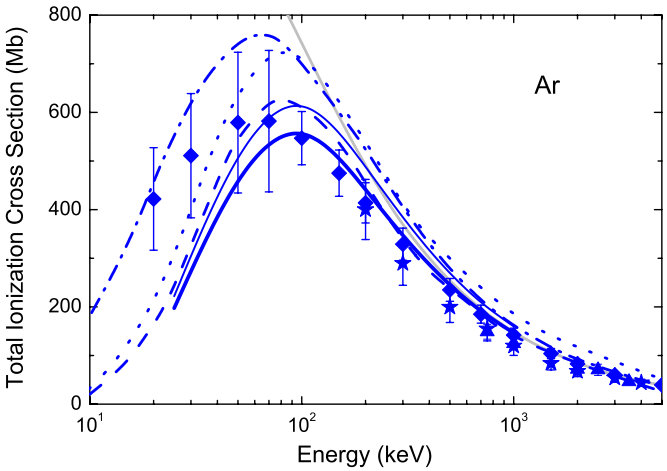

Figure A1. Total ionization cross section of Ar by proton impact. Curves: thick solid line, CDW-EIS; thin solid line, previous CDW-EIS [67]; dashed line, CDW-EIS with the optimized potential method (OPM) by Gulyas and Kirchner [106]; dotted line, CDW-EIS with the Hartre–Fock–Slater model potential [107]; dashed-dotted line, BGM with OPM including target response [106]. Experimental data for proton impact by DuBois *et al* [2], Cavalcanti *et al* [57] and Rudd *et al* [83]. Symbols are given in figure 2.

the impact parameter $\vec{b} = \{b, \varphi_b\}$ can be related to the corresponding amplitudes $P(E, \Omega, \vec{b}) = |a(E, \Omega, \vec{b})|^2$ where

$$a(E, \Omega, \vec{b}) = \sum_{m=-M}^{M} i^m \frac{\exp(im\,\varphi_b)}{\sqrt{2\pi}} a_m(E, \Omega, b), \qquad (A.2)$$

with

$$a_m(E, \Omega, b) = i^{-m} \int_0^\infty \eta\, d\eta\, J_m(b\eta) T_m(E, \Omega, \eta). \qquad (A.3)$$

The key magnitude is then $T_m(E, \Omega, \eta)$ which can be calculated with the inverse Fourier transform of equation (A.1):

$$T_m(E, \Omega, \eta) = i^{-m} \int_0^{2\pi} d\varphi_\eta \frac{\exp(-im\,\varphi_\eta)}{\sqrt{2\pi}} T(E, \Omega, \eta, \varphi_\eta). \qquad (A.4)$$

In this paper, we used a cubic spline to represent $T(E, \Omega, \eta, \varphi_\eta)$, which permits us to obtain a closed form for the integral including the factor $\exp(-im\,\varphi_\eta)$. Instead, in [67] we used a numerical quadrature technique with $(2l_{\max} + 1)$ Gauss Legendre pivots to calculate equation (A.4). It was not accurate enough, giving probabilities $P(E, \Omega, \vec{b})$ erroneously small at small impact parameters and too large at large impact parameters. However, the b-integrated cross sections remain the same, within a few per cent.

In figure A1, we display the total ionization cross section for protons in Ar. In this figure, we perform a comparison of present CDW-EIS results with those obtained from [67]. Also in figure A1 we compare it with other theoretical results [106, 107] (using the CDW-EIS model but different potentials, and with the TDSE-BGM) [106]. It can be noted that the difference between present improved CDW-EIS results and the previous ones in [67] is less than with other CDW-EIS calculations with different potential. The high-energy description of the proton–Ar data by present CDW-EIS results is very good.

Multiple-ionization cross sections are very sensitive to the $P(E, \Omega, \vec{b})$ at small values of b; for this reason, the values in [67] for double to quintuple ionization are erroneously small, specially at low-impact energies.

Present multiple-ionization cross sections, with both CDW-EIS and first Born approximations, are larger than those of [67] for energies below 1 MeV. They correct the (suspicious) agreement of Born values with the experimental data at low energies obtained in [67]. In fact, present Born results are definitively larger than the experiments in the intermediate energy region, as one would expect.

References

[1] DuBois R D 1984 *Phys. Rev. Lett.* **52** 2348–51
[2] DuBois R D, Toburen L H and Rudd M E 1984 *Phys. Rev.* A **29** 70–6
[3] DuBois R D 1987 *Phys. Rev.* A **36** 2585–93
[4] DuBois R D 1989 *Phys. Rev.* A **39** 4440–50
[5] DuBois R D and Manson S T 1987 *Phys. Rev.* A **35** 2007–25
[6] DuBois R D and Manson S T 1987 *J. Physique* **48** C9 263–6
[7] Lüdde J H L and Dreizler R 1985 *J. Phys. B: At. Mol. Opt. Phys.* **18** 107
[8] McGuire J H 1997 *Electron Correlation Dynamics in Atomic Collisions* (Cambridge: Cambridge University Press)
[9] Shevelko V and Tawara H 1998 *Atomic Multielectron Processes* (Berlin: Springer)
[10] Kirchner T and Knudsen H 2011 *J. Phys. B: At. Mol. Opt. Phys.* **44** 122001
[11] Andersen L H, Hvelplund P, Knudsen H, Möller S P, Elsener K, Rensfelt K G and Uggerhöj E 1986 *Phys. Rev. Lett.* **57** 2147–50
[12] Andersen L H, Hvelplund P, Knudsen H, Möller S P, Sörensen A H, Elsener K, Rensfelt K G and Uggerhöj E 1987 *Phys. Rev.* A **36** 3612–29
[13] Andersen L H, Hvelplund P, Knudsen H, Möller S P, Pedersen J O P, Tang-Pedersen S, Uggerhöj E, Elsener K and Morenzoni E 1989 *Phys. Rev.* A **40** 7366
[14] Paludan K, Bluhme H, Knudsen H, Mikkelsen U, Möller S P, Uggerhöj E and Morenzoni E 1997 *J. Phys. B: At. Mol. Opt. Phys.* **30** 3951
[15] Knudsen H *et al* 2008 *Phys. Rev. Lett* **101** 043201
[16] Knudsen H *et al* 2009 *Nucl. Instrum Methods Phys. Res.* B **267** 244–7
[17] Knudsen H and Reading J F 1992 *Phys. Rep.* **212** 107–222
[18] Schultz D R, Olson R E and Reinhold C O *J. Phys. B: At. Mol. Opt. Phys.* **24** 521–58
[19] de Heer F J, Jansen R H J and van der Kaay W 1979 *J. Phys. B: At. Mol. Opt. Phys.* **12** 979–1002
[20] Defrance P, Jureta J J, Kereselidze T, Lecointre J and Machavariani Z S 2009 *J. Phys. B: At. Mol. Opt. Phys.* **42** 025202
[21] Schram B L, de Heer F J, Van der Wiel M J and Kistermaker J 1965 *Physica* **31** 94
[22] Schram B L, Boerboom A J H and Kistermaker J 1966 *Physica* **32** 185–96
Schram B L 1966 *Physica* **32** 197–209
[23] Adamczyk B, Boerboom A J H, Schram B L and Kistermaker J 1966 *J. Chem. Phys.* **44** 4640–2
[24] Krishnakumar E and Srivastava S K 1988 *J. Phys. B: At. Mol. Opt. Phys.* **21** 1055–82
[25] Nagy P, Skutlartz A and Schmidt V 1980 *J. Phys. B: At. Mol. Opt. Phys.* **13** 1249–67

[26] Kirchner T, Horbatsch M, Wagner E and Lüdde H J 2002 *J. Phys. B: At. Mol. Opt. Phys.* **35** 925–34
[27] Lopez S D, Garibotti C R and Otranto S 2011 *Phys. Rev.* A **83** 062702
[28] Igarashi A, Ohsaki A and Nakazaki S 2000 *Phys. Rev.* A **62** 052722
[29] Pinzola M S, Lee T G and Colgan J 2011 *J. Phys. B: At. Mol. Opt. Phys.* **44** 205204
[30] Foster M, Colgan J and Pinzola M S 2008 *J. Phys. B: At. Mol. Opt. Phys.* **41** 111002
[31] Guan X and Bartschat K 2009 *Phys. Rev. Lett.* **103** 213201
[32] Abdurakhmanov I B, Kadyrov A S, Fursa D V, Bray I and Stelbovics A T 2011 *Phys. Rev.* A **84** 062708
[33] Carlson T A and Krause M O 1965 *Phys. Rev.* **140** A1057
[34] Carlson T A, Hunt W E and Krause M O 1966 *Phys. Rev.* **151** 41
[35] Krause M O, Vestal M V, Johnson W H and Carlson T A 1964 *Phys. Rev.* **133** A385
[36] Carlson T A and Krause M O 1965 *Phys. Rev. Lett.* **14** 390
[37] Carlson T A and Krause M O 1965 *Phys. Rev.* **137** A1655
[38] Krause M O and Carlson T A 1966 *Phys. Rev.* **149** 52
[39] Landers A L *et al* 2009 *Phys. Rev. Lett.* **102** 223001
[40] Morgan D V, Sagurton M and Bartlett R J 1997 *Phys. Rev.* A **55** 1113
[41] Morishita Y *et al* 2006 *J. Phys. B: At. Mol. Opt. Phys.* **39** 1323
[42] Armen G B, Kanter E P, Krässig B, Levin J C, Southworth S H and Young L 2004 *Phys. Rev.* A **69** 062710
[43] Saito N and Suzuki I H 1992 *Phys. Scr.* **45** 253
[44] Tamenori Y *et al* 2002 *J. Phys. B: At. Mol. Opt. Phys.* **35** 2799
[45] Tamenori Y *et al* 2004 *J. Phys. B: At. Mol. Opt. Phys.* **37** 117
[46] Brünken S *et al* 2002 *Phys. Rev.* A **65** 042708
[47] Viefhaus J *et al* 2004 *Phys. Rev. Lett.* **92** 083001
[48] Hikosaka Y *et al* 2007 *Phys. Rev.* A **76** 032708
[49] Hayaishi T *et al* 1990 *J. Phys. B: At. Mol. Opt. Phys.* **23** 4431
[50] Karmmerling B, Krassig B and Schmidt V 1992 *J. Phys. B: At. Mol. Opt. Phys.* **25** 3621
[51] Hayaishi T, Matsui T, Yoshii H, Higurashi A, Murakami E, Yagishita A, Aoto T, Onuma T and Morioka Y 2002 *J. Phys. B: At. Mol. Opt. Phys.* **35** 141
[52] Hikosaka Y, Aoto T, Lablaniquie P, Penent F, Shigemasa E and Ito K 2006 *J. Phys. B: At. Mol. Opt. Phys.* **39** 3457
[53] Matsui T, Yoshii H, Tsukamoto K, Kawakita S, Murakami E, Adachi J, Yagishita A, Morioka Y and Hayaishi T 2004 *J. Phys. B: At. Mol. Opt. Phys.* **37** 3745
[54] Santos A C F, Melo W S, Sant 'Anna M M, Sigaud G M and Montenegro E C 2001 *Phys. Rev.* A **63** 062717
[55] Cavalcanti E G, Sigaud G M, Montenegro E C, Sant 'Anna M M and Schmidt-Bocking H 2002 *J. Phys. B: At. Mol. Opt. Phys.* **35** 3937
[56] Spranger T and Kirchner T 2004 *J. Phys. B: At. Mol. Opt. Phys.* **37** 4159
[57] Cavalcanti E G, Sigaud G M, Montenegro E C and Schmidt-Bocking H 2003 *J. Phys. B: At. Mol. Opt. Phys.* **36** 3087
[58] Sant'Anna M M, Luna H, Santos A C F, McGrath C, Shah M B, Cavalcanti E G, Sigaud G M and Montenegro E C 2003 *Phys. Rev.* A **68** 042707
[59] Sigaud G M, Sant' Anna M M, Luna H, Santos A C F, McGrath C, Shah M B, Cavalcanti E G and Montenegro E C 2004 *Phys. Rev.* A **69** 062718
[60] Wolff W, Luna H, Santos A C F, Montenegro E C and Sigaud G M 2009 *Phys. Rev.* A **80** 032703
[61] Kirchner T, Santos A C F, Luna H, Sant'Anna M M, Melo W S, Sigaud G M and Montenegro E C 2005 *Phys. Rev.* A **72** 012707
[62] Galassi M E, Rivarola R D and Fainstein P D 2007 *Phys. Rev.* A **75** 052708
[63] Tachino C A, Galassi M E and Rivarola R D 2008 *Phys. Rev.* A **77** 032714
[64] Tachino C A, Galassi M E and Rivarola R D 2009 *Phys. Rev.* A **80** 014701
[65] Schenk G and Kirchner T 2009 *J. Phys. B: At. Mol. Opt. Phys.* **42** 205202
[66] Archubi C D, Montanari C C and Miraglia J E 2007 *J. Phys. B: At. Mol. Opt. Phys.* **40** 943
[67] Montanari C C, Montenegro E C and Miraglia J E 2010 *J. Phys. B: At. Mol. Opt. Phys.* **43** 165201
[68] Montanari C C, Wolff W, Luna H, Santos A C F, Montenegro E C and Miraglia J E 2012 Multiple ionization of atoms including post-collisional contributions *Proc. 27th Int. Conf. on Photonic, Electronic and Atomic Collisions (Belfast, August 2011)*; 2012 *J. Phys: Conf. Ser.* to be published
[69] Wolff W, Luna H, Santos A C F, Montenegro E C, DuBois R D, Montanari C C and Miraglia J E 2011 *Phys. Rev.* A **84** 042704
[70] Kirchner T, Lüdde H J and Dreizler R M 1999 *Phys. Rev.* A **61** 012705
[71] Kirchner T, Horbatsch M and Lüdde H J 2002 *Phys. Rev.* A **66** 052719
[72] Crothers D S F and McCann J F 1983 *J. Phys. B: At. Mol. Opt. Phys.* **16** 3229
[73] Fainstein P D, Ponce V H and Rivarola R D 1988 *J. Phys. B: At. Mol. Opt. Phys.* **21** 287–99
[74] Rivarola R D, Fainstein P D and Ponce V H 1989 *Proc. 16th Int. Conf. on the Physics of Electronic and Atomic Collisions* ed A Dalgarno *et al* (New York: AIP) p 264
[75] Miraglia J E and Gravielle M S 2008 *Phys. Rev.* A **78** 052705
[76] Miraglia J E 2009 *Phys. Rev.* A **79** 022708
[77] Miraglia J E and Gravielle M S 2010 *Phys. Rev.* A **81** 042709
[78] Fainstein P D, Ponce V H and Rivarola R D 1989 *J. Phys. B: At. Mol. Opt. Phys.* **22** L559–63
[79] Fainstein P D, Ponce V H and Rivarola R D 1988 *J. Phys. B: At. Mol. Opt. Phys.* **21** 2989–98
[80] Fainstein P D, Ponce V H and Rivarola R D 1987 *Phys. Rev.* A **36** 3639–41
[81] Rapp D and Englander-Golden P 1965 *J. Chem. Phys.* **43** 1464
[82] Tawara H and Kato T 1987 *At. Data Nucl. Data Tables* **36** 167
[83] Rudd M E, Kim Y-K, Madison D H and Gallagher J W 1985 *Rev. Mod. Phys.* **57** 965–94
[84] Sorokin A A, Shmaenok L A, Bobashev S V, Möbus B, Richter M and Ulm G 2000 *Phys. Rev.* A **61** 022723
[85] Sant'Anna M M, Montenegro E C and McGuire J H 1998 *Phys. Rev.* A **58** 2148–59
[86] Kochur A G, Sukhorukov V L, Dudenko A I and Demekhin P V 1995 *J. Phys. B: At. Mol. Opt. Phys.* **28** 387
[87] Gonzalez A D and Horsdal Pedersen E 1993 *Phys. Rev.* A **48** 3689
[88] Haugen H K, Andersen L H, Hvelplund P and Knudsen H 1982 *Phys. Rev.* A **26** 1962–74
[89] Rejoub R, Lindsay B G and Stebbing R F 2002 *Phys. Rev.* A **65** 042713
[90] Kobayashi A, Fujiki G, Okaji A and Masuoka T 2002 *J. Phys. B: At. Mol. Opt. Phys.* **35** 2087–103
[91] McCallion P, Shah M B and Gilbody H B 1992 *J. Phys. B: At. Mol. Opt. Phys.* **25** 1061–71
[92] Straub H C, Renault P, Lindsay B G, Smith K A and Stebbings R F 1995 *Phys. Rev.* A **52** 1115–24
[93] El-Sherbini T, van der Wiel M J and de Heer F J 1970 *Physica* **48** 157–64
[94] Syage J A 1992 *Phys. Rev.* A **46** 5666
[95] Jha L K, Kumar S and Roy B N 2006 *Eur. Phys. J.* D **40** 101–6
[96] Carlson T A and Nestor C W Jr 1973 *Phys. Rev.* A **8** 2887–93

[97] Carlson T A, Nestor C W Jr, Tucker T C and Malik F B 1968 *Phys. Rev.* **169** 27–36
[98] Mukoyama T 1978 *Acta Phys. Hung.* **44** 187
[99] Mukoyama T and Taniguchi K 1987 *Phys. Rev* A **36** 693–8
[100] Kochur A G and Popov V A 2006 *Rad. Phys. Chem.* **75** 1525–8
[101] Mohammedein A D, Ghoneim A A, Al-Zanki J M, Altouq M S and El-Essawy A H 2010 *Adv. Studies Theor. Phys.* **4** 55–66
[102] Bartlett P L and Stelbovits A T 2002 *Phys. Rev.* A **66** 012707
[103] Naghma R, Mahato B N, Vinodkumar M and Antony B K 2011 *J. Phys. B: At. Mol. Opt. Phys.* **44** 105204
[104] Gilbody H B and Hasted J B 1957 *Proc. R. Soc.* A **240** 382
[105] Rudd M E, DuBois R D, Toburen L H, Ratcliffe C A and Goffe T V 1983 *Phys. Rev.* A **28** 3244
[106] Gulyas L and Kirchner T 2004 *Phys. Rev.* A **70** 022704
[107] Kirchner T, Gulyas L, Lüdde H J, Henne A, Engel E and Dreizler R M 1997 *Phys. Rev. Lett.* **79** 1659